CALCULATION OF A LAMINAR BOUNDARY LAYER ON THE LEEWARD SIDE OF A TRIANGULAR PLATE WITH SUPERSONIC LEADING EDGES

V. N. Vetultskii and T. V. Poplavskaya

UDC 532.526

In a supersonic flow about a conical body with an angle of attack which is less than the limiting value, the inviscid flow behind the shock wave (SW) is conical. The laminar boundary layer on such a body is described by equations dependent on two similarity variables [1]. This formulation of the problem was used to examine a boundary layer on the windward side of a triangular plate in [2-5]. A large number of experimental studies [6-8] have qualitatively examined flow regimes on the leeward side of a triangular plate with different Mach numbers and angles of attack. The heat-transfer coefficients on the leeward side of a delta wing with an angle of sweep $\chi = 80°$ was measured in [9] at $M_\infty = 10$ and different angles of attack. Here, all of the variants correspond to a flow regime in which shock waves are shed from the edges. An incompressible three-dimensional boundary layer on the leeward side of a delta wing was calculated in [10, 11], where the theoretical region was located between the attachment line and the convergence line of the vortex.

Here, we find the parameters of a laminar boundary layer on the leeward side of a triangular plate in the case where a shock wave is attached to the leading edges. The solution of the similarity equations is constructed from the leading edge by the flight method. The solution is constructed to the generatrix, where transverse separation begins. Then the similarity equations of the boundary layer are augmented by the second derivatives of the sought functions in the circumferential direction, and the problem is solved in the separation region by the establishment method.

1. We will examine supersonic flow about a triangular plate at the angle of attack α. The velocity vector of the incoming flow lies in the plane of symmetry. In the case of supersonic leading edges, the flows on the upper and lower sides of the plate do not affect each other and can be calculated independently. In the neighborhood of the edge, the inviscid flow is rotated in the Prandtl—Mayer flow with slip, and the parameters of the gas have constant values after the last characteristic. The flow then changes to a conical stream of general form. This transition is accompanied by a sharp pressure increase and, possibly, by the creation of an internal shock wave [12-14].

On the leeward side of the plate, we introduce a cylindrical coordinate system (r, θ, z) similar to [3]. Here, r is the distance along the generatrix of the plate; θ is the angle between the generatrix and the plane of symmetry; z is the normal to the surface of the plate. Analogously to the windward side, the boundary-layer equations allow a similarity solution which is dependent on the variables $\omega = \theta_0 - \theta, \eta = z/\sqrt{r(\theta_0 - \theta)}$ (θ_0 is the angle of the leading edge). Equations in similarity variables can be solved by the flight method along the coordinate ω in the direction of the transverse component of velocity v. In the regime being examined here, as from the windward side, flow on the external boundary of the boundary layer on the leeward side is directed from the leading edges to the plane of symmetry. Thus, to use the flight method, it is necessary to assign initial conditions in the neighborhood of the leading edge. As ω approaches zero, the equations in the similarity variables become ordinary differential equations whose solution is used as initial data [3].

Similarity boundary-layer equations in the variables ω and η are solved on the windward side over the entire surface of the plate [3]. The solution is similarly constructed on the leeward side, from the leading edge to a certain generatrix behind which the transverse velocity component changes sign near the wall. Here, the region of flow separation begins to form in the transverse direction. The solution of similarity boundary-layer equations cannot be continued along the ω coordinate when the flight method is used. By virtue of the

Novosibirsk. Translated from Zhurnal Prikladnoi Mekhaniki i Tekhnicheskoi Fiziki, No. 1, pp. 75-81, January-February, 1988. Original article submitted October 13, 1987.

0021-8944/89/3001-0071$12.50

TABLE 1

χ°	M_∞	α°	c_F^*	Q_T^*
45	4	5	1,374 1,375	0,722 0,723
55	4	5	— 1,382	— 0,727
60	4	5	— 1,448	— 0,747
45	2	5	1,720 1,722	0,933 0,933
45	3	5	1,530 1,532	0,814 0,815
45	4	5	1,374 1,375	0,722 0,723
45	6	5	— 1,137	— 0,587
45	3	5	1,530 1,532	0,814 0,815
45	3	10	— 1,286	— 0,665
45	3	15	— 1,108	— 0,553

principle of influence and dependence for a three-dimensional boundary layer [15], we need to formulate and solve an independent boundary-value problem for the ω coordinate.

Following [16], we added unordered terms containing second derivatives of the sought flow parameters with respect to ω to the similarity boundary-layer equations in the transverse separation region. These terms can be regarded as terms having artificial viscosity. With allowance for the conversion of the variables to dimensionless form and execution of the transformations described in [3], the system of equations has the form

$$\frac{f'}{L}\frac{\partial J}{\partial \xi}+\omega\left(\frac{3}{2}\rho u-\frac{\partial \rho v}{\partial \omega}\right)-\frac{f'}{L}\frac{L'}{L}\omega\rho vN-\frac{1}{2}\rho v=0,$$

$$\frac{f'}{L}J\frac{\partial u}{\partial \xi}-\omega\rho v\left(\frac{\partial u}{\partial \omega}+v\right)-\frac{f'}{L}\frac{\partial}{\partial \xi}\left(\mu\frac{f'}{L}\frac{\partial u}{\partial \xi}\right)-\delta\omega\frac{\partial}{\partial \omega}\left(\mu\frac{\partial u}{\partial \omega}\right)=$$

$$=-\omega\rho_e v_e\left(\frac{\partial u_e}{\partial \omega}+v_e\right)-\delta\omega\frac{\partial}{\partial \omega}\left(\mu_e\frac{\partial u_e}{\partial \omega}\right),$$

$$\frac{f'}{L}J\frac{\partial v}{\partial \xi}+\omega\rho v\left(u-\frac{\partial v}{\partial \omega}\right)-\frac{f'}{L}\frac{\partial}{\partial \xi}\left(\mu\frac{f'}{L}\frac{\partial v}{\partial \xi}\right)-\delta\omega\frac{\partial}{\partial \omega}\left(\frac{4}{3}\mu\frac{\partial v}{\partial \omega}\right)=$$

$$=\omega\rho_e v_e\left(u_e-\frac{\partial v_e}{\partial \omega}\right)-\delta\omega\frac{\partial}{\partial \omega}\left(\frac{4}{3}\mu_e\frac{\partial v_e}{\partial \omega}\right), \qquad (1.1)$$

$$c_p J\frac{f'}{L}\frac{\partial T}{\partial \xi}-c_p\rho v\omega\frac{\partial T}{\partial \omega}-\frac{f'}{L}\frac{1}{\mathrm{Pr}}\frac{\partial}{\partial \xi}\left(\frac{f'}{L}k\frac{\partial T}{\partial \eta}\right)-\frac{1}{\mathrm{Pr}}\delta\omega\frac{\partial}{\partial \omega}\left(k\frac{\partial T}{\partial \omega}\right)=-c_{p_e}\rho_e v\omega\frac{\partial T_e}{\partial \omega}-$$

$$-\frac{1}{\mathrm{Pr}}\delta\omega\frac{\partial}{\partial \omega}\left(k_e\frac{\partial T_e}{\partial \omega}\right)+(\gamma-1)M_\infty^2\mu\left(\frac{f'}{L}\right)^2\left[\left(\frac{\partial u}{\partial \xi}\right)^2+\left(\frac{\partial v}{\partial \xi}\right)^2\right],\quad p=\frac{1}{\gamma M_\infty^2}\rho T.$$

The problem was solved with the following boundary conditions:

$$\omega=\omega_+:\ u=u_+(\xi),\ v=v_+(\xi),\ T=T_+(\xi),$$

$$\omega=\theta_0:\ \partial u/\partial\omega=0,\ v=0,\ \partial T/\partial\omega=0, \qquad (1.2)$$

$$\xi=0:\ u=v=J=0,\ T=T_w,$$

$$\xi=1:\ u=u_e(\omega),\ v=v_e(\omega),\ T=T_e(\omega),\ p=p_e(\omega).$$

Here, ξ is the logarithmic extension of the normal coordinate η [1, 5]:

$$\xi=f(\eta/L)=\ln\,(1+\eta/\varepsilon_2 L)/\ln\,(1+1/\varepsilon_2)$$

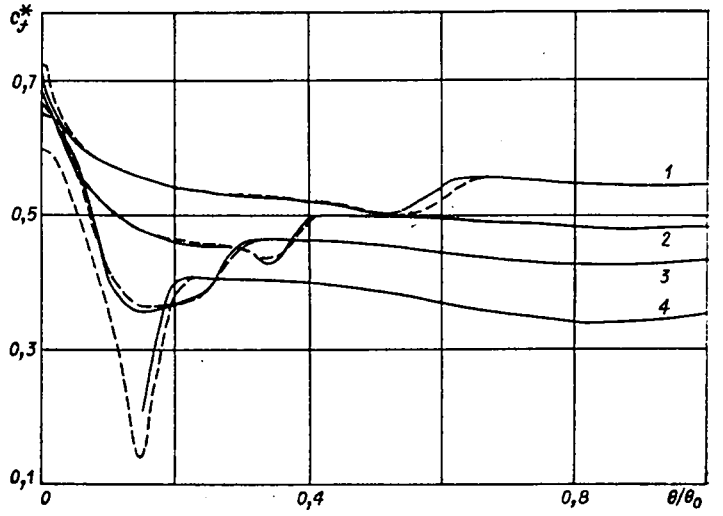

Fig. 1

($L = L(\omega)$ is the theoretical thickness of the boundary layer). Also, instead of the normal component of velocity w, we introduce the mass velocity J and the function $N(\omega, \xi)$: $J = \rho\sqrt{\omega}\left(-0.5\eta u + \sqrt{\omega}\frac{L'}{L}\eta v + w\sqrt{r}\right) + 0.5\rho\eta v$, $N = \partial\eta/\partial\xi = L(\omega)\varepsilon_2(1 + 1/\varepsilon_2)^{\xi}\ln(1 + 1/\varepsilon_2)$. All of the flow parameters are referred to their values in the incoming flow, while pressure is referred to the doubled velocity head $\rho_\infty U_\infty^2$.

The profiles of $u_+(\xi)$, $v_+(\xi)$, $T_+(\xi)$ were taken from the solution of the boundary layer equations obtained by the flight method with $\omega = \omega_+$. We took the distributions $p_e(\omega)$ and $v_e(\omega)$ from the calculation of inviscid flow on the external boundary of the boundary layer ($\xi = 1$). We then used these distributions, the Bernoulli integral, and the entropy on the plate surface to calculate the distributions $u_e(\omega)$ and $T_e(\omega)$:

$$u_e = \left(2\gamma/(\gamma-1)(1 - p_e/\rho_e) - \gamma M_\infty^2 - v_e^2\right)^{1/2},\quad T_e = p_e/\rho_e,\quad \rho_e = (p_e/S)^{\gamma_1},\quad \gamma_1 = 1/\gamma \tag{1.3}$$

(all of the parameters were made dimensionless, as in [13]).

Strictly speaking, with the introduction of unordered terms containing a second derivative into system (1.1), its solution should depend on the local Reynolds number, since the coefficient δ is equal to 1/Re. Calculations performed with $\chi = 45°$, $M_\infty = 4$, and $\alpha = 5°$ showed that a change in δ from 10^{-4} to 10^{-5} gives a difference of no more than 6% in the friction and heat-transfer coefficient, while a change from 10^{-5} to 10^{-6} gives a difference of less than 1%. The result calculated for $\delta = 0$ nearly coincides with the result obtained for $\delta = 10^{-5}$. All this indicates that the solution of system (1.1) can be considered nearly self-similar and independent of Re at small values of δ.

2. System (1.1) was solved by the establishment method. Here, we added a nonsteady term to each equation of the system. Thus, both equations of motion and the energy equation can be written in the form

$$\frac{\partial F}{\partial t} + a\frac{\partial F}{\partial \omega} + b\frac{\partial F}{\partial \xi} + e\frac{\partial}{\partial \xi}\left(c\frac{\partial F}{\partial \xi}\right) + s\frac{\partial}{\partial \omega}\left(g\frac{\partial F}{\partial \omega}\right) + d = 0, \tag{2.1}$$

where F signifies u, v, and T. The specific heat capacity c_p was assumed to be constant, while the viscosity coefficient and thermal conductivity were approximated with an exponential relation $\mu = T^{0.76}$, $k = T^{0.76}$. System (2.1) was solved numerically by means of an implicit two-level difference scheme along the coordinate ξ. The derivatives with respect to the coordinate ω were taken from the previous iteration. The first derivative with respect to ω was determined by means of a second-order angle scheme in relation to the direction of transverse flow [17]. All of the coefficients of the equations were taken from the previous iteration of the new level. One iteration was performed at each time level. On the whole, the scheme employed was characterized by the second order of approximation with respect to the steady-state solution. The continuity equation was associated with the same degree of accuracy.

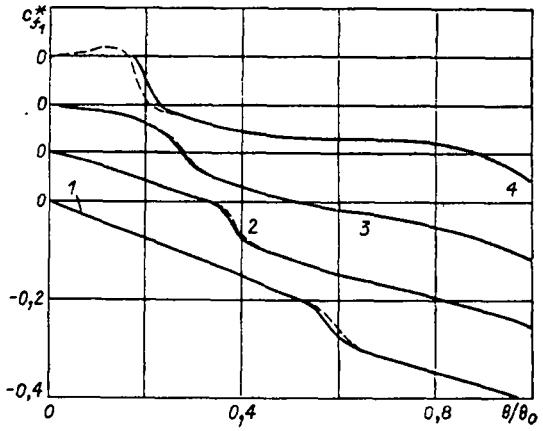

Fig. 2

First we constructed the solution of the "parabolic" problem (without second derivatives with respect to the coordinate ω) from the leading edge $\omega = 0$ to the ray $\omega = \omega_+$, where the profile of the transverse component of velocity v_+ approached the pre-separation profile. Then, for "elliptical" problem (1.1), (1.2), we calculated the initial approximation. For this, the profiles $u_+(\xi)$, $v_+(\xi)$, and $T_+(\xi)$ were recalculated for all subsequent rays up to the plane of symmetry $\omega = \theta_0$ and were normalized with respect to their values on the external boundary for the given ray. Then, for the region $\omega_+ < \omega \leqslant \theta_0$, we solved the "elliptical" problem (1.1), (1.2) until the steady state was attained.

Numerical solution of the "elliptical" problem allowed us to determine the profiles of velocity and temperature in the boundary layer on the leeward side of the plate. We then used these profiles for the surface of the body to calculate the local shear-stress coefficients in the longitudinal c_{f_1} and transverse c_{f_2}, the absolute value of the vector of the local friction coefficient $c_f = (c_{f_1}^2 + c_{f_2}^2)^{1/2}$, and the local heat-transfer coefficient St (Stanton number). All of these quantities were referred to the velocity head of the incoming flow and were determined from formulas presented in [5]. However, these parameters are difficult to show graphically, since they tend to infinity with the approach of the leading edges of the plate and its tip. Also, they are dependent on the local Re. Thus, for greater convenience in calculating and representing them, we used local similarity parameters dependent only on ω:

$$c^*_{f_1} = c_{f_1}\sqrt{\mathrm{Re}_r\omega}, \quad c^*_{f_2} = c_{f_2}\sqrt{\mathrm{Re}_r\omega}, \quad c^*_f = c_f\sqrt{\mathrm{Re}_r\omega}, \quad \mathrm{St}^* = \mathrm{St}\sqrt{\mathrm{Re}_r\omega},$$

where Re_r is the local Reynolds number, calculated from the parameters of the incoming flow and the distance along the generatrix of the plate r.

Besides the local friction and heat-transfer coefficients on the leeward side of the plate, we obtained the overall similarity friction coefficient $c_F^* = c_F\sqrt{\mathrm{Re}_l}$ and the heat flux $Q_T^* = Q_T\sqrt{\mathrm{Re}_l}$. These two quantities were referred to the area of the plate [5] (Re_l is the Reynolds number determined from the length of the central chord l).

3. Table 1 shows the results of calculations of the parameters of a laminar boundary layer on the lee side of a triangular plate. The calculations were performed for several values of χ, M_∞, and α. In all of the variants, the ratio of the enthalpy of the wall H_w to the total enthalpy of the incoming flow H_∞ was taken equal to 0.1, Pr = 0.7, $\delta = 10^{-3}$.

The conditions on the external boundary of the layer were taken from the table in [13]. It should be noted that the parameters of the inviscid flow on the lee side have small oscillations in the region of high gradients. We smoothed them in the present calculations.

It is known that flow in the neighborhood of the separation point is very sensitive to small perturbations of any character. Thus, the error of the calculations also increases sharply in this region. In the solution of the "parabolic" problem, we took the largest number of steps along the normal to the plate (40) and with respect to the angular coordinate (160). In this case, the error of the calculations of c_f^* and St* was hundredths of a percent everywhere except for the pre-separation region, where it reached several percent. As the parameter δ approached zero in the "elliptical" problem, its solution approached the solution of the "parabolic" problem (Figs. 1-3). However, the difference was still

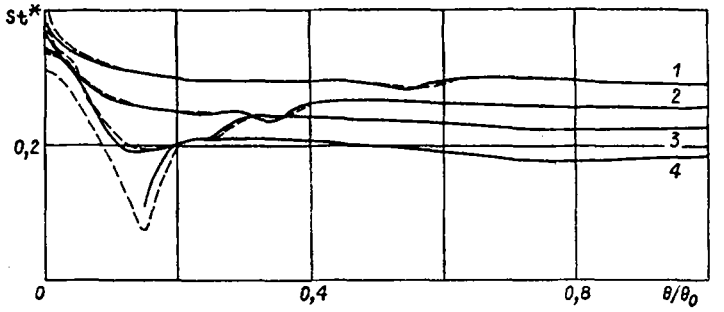

Fig. 3

substantial in the pre-separation region in several of the variants (Figs. 4 and 5). Here, it should be kept in mind that different difference schemes were used to solve the "parabolic" and "elliptical" problems.

Figures 1-3 show distributions of the parameters c_f^*, c^*f_2 and St* on the lee surface of the plate for $\chi = 45°$, $\alpha = 5°$ and $M_\infty = 2, 3, 4, 6$ (curves 1-4). The solid lines in all of the figures correspond to the "parabolic" problem, while the dashed lines correspond to the "elliptical" problem. It is evident that in the region of the leading edge, where the inviscid flow is constant, the values of c_f^* and St* remain nearly constant. The inviscid flow then undergoes restructuring and pressure increases sharply, which causes stagnation of the boundary layer in the transverse direction. At $M_\infty = 6$, this stagnation leads to a change in the sign of the transverse velocity component v near the plate surface. Thus, the solution of the parabolic problem cannot be continued beyond $\theta/\theta_0 = 0.12$. The solution of the elliptical problem yields transverse separation in this region, which is quite evident from Fig. 2. The solutions of both problems are close for this variant outside the separation region and for the other three Mach numbers throughout the entire region. The exception is the plane of symmetry, in the neighborhood of which there is a substantial difference in the parameters c_f^* and St* obtained in the solution of both problems. This can be attributed to the fact that symmetry conditions (1.2) are imposed in the solution of the elliptical problem in the plane of symmetry ($\omega = \theta_0$), while there are no boundary conditions here in the solution of the parabolic problem. A similar difference is seen for the lee side of a circular cone [16].

Figure 4 shows the distribution of the parameter c_f^* on the lee side of the plate with $M_\infty = 4$, $\alpha = 5°$ and $\chi = 45, 55, 60°$ (curves 1-3). It is evident that the angle of sweep depends slightly on the value of c_f^* in the region of uniform inviscid flow. This difference increases in the region where pressure increases, and at $\chi = 55$ and 60° the pressure gradient leads to transverse separation of the boundary layer.

Figure 5 shows the distribution of the parameter c_f^* in relation to the angle θ. Here, $\chi = 45°$, $M_\infty = 3$ and $\alpha = 5, 10, 15°$ (curves 1-3). In the region of uniform inviscid flow, the value of c_f^* decreases by one-third with an increase in α from 5 to 15°. The pressure gradient on the leeward side increases in this case, which also helps explain the transverse separation at $\alpha = 10$ and 15°.

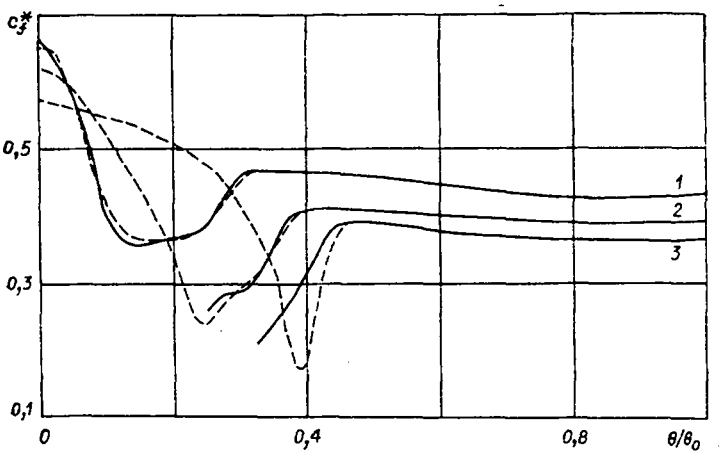

Fig. 4

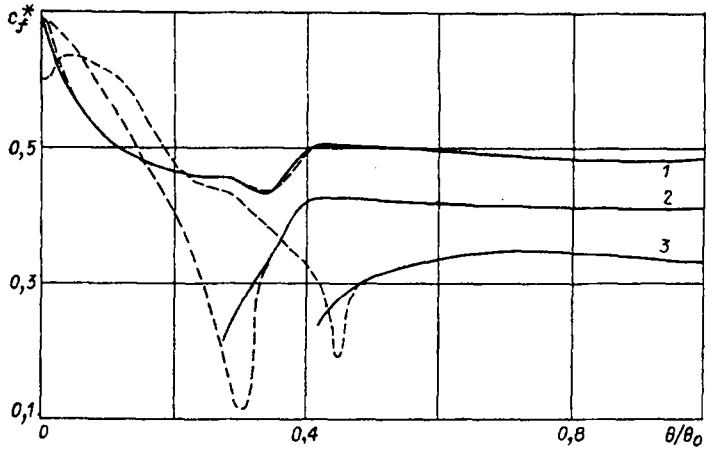

Fig. 5

A change in the angle of sweep and angle of attack affects the similarity value of St* as it does c_f^*. Here, no increase in local heat transfer is seen in the region of transverse separation.

It should be noted that the transverse separation seen in the present investigation means that eddies will appear in the boundary layer on the lee side of the plate. Using Narayan's terminology [9], such eddies are called "submerged" eddies, in contrast to the eddies which envelop the inviscid flow. In the latter case, flows of high-enthalpy gas from the inviscid region move along the line of attachment of the eddy on the surface of the body, which causes an increase in local heat flows in this region.

4. Table 1 shows the overall values of the similarity friction coefficient c_F^* and heat flux Q_T^* on the lee side of the plate. The top number in each column corresponds to the parabolic problem, while the bottom number corresponds to the elliptical problem. The lines denote that the parabolic problem cannot be solved to the plane of symmetry for the given variant due to transverse separation. It is evident from the ›le that a change in χ in the investigated range has almost no effect on c_F^* and Q_T^*. A similar pattern was observed on the windward side of a plate in [5].

The value of c_F^* on the lee side decreases almost linearly with an increase in M_∞, although it increased with M_∞ on the windward side in [5]. Thus, the contribution of the lee side to the overall friction coefficient of the plate decreases from 47 to 34% with an increase in M_∞ from 2 to 6 at $\chi = 45°$ and $\alpha = 5°$.

The dependence of the parameter c_F^* on α on the lee side decreases monotonically, while the reverse is seen on the windward side [5]. This and the previous phenomenon can apparently be explained by the fact that an increase in α or M_∞ is accompanied by a decrease in the density of the gas on the lee side and an increase in gas density on the windward side. The contribution of the lee side to the overall friction coefficient of the plate decreases from 43 to 31% with an increase in α from 5 to 15° at $\chi = 45°$ and $M_\infty = 3$.

LITERATURE CITED

1. N. D. Vvedenskaya, "Calculation of the boundary layer which develops in flow about a cone with an angle of attack," Zh. Vychisl. Mat. Mat. Fiz., 6, No. 2 (1966).
2. V. A. Bashkin, "Laminar boundary layer in a compressible gas with conical external flow," Tr. Tsentr. Aerogidrod. Inst., No. 1093 (1968).
3. V. N. Vetlutskii and T. V. Poplavskaya, "Calculation of the laminar boundary layer on a flat triangular plate with supersonic leading edges," ChMMSS, 13, No. 1 (1982).
4. V. N. Vetlutskii and T. V. Poplavskaya, "Tables of parameters for a laminary boundary layer on the windward side of a flat triangular plate in a streamline flow regime with a shock wave attached to the edge," Preprint, Inst. Teor. Prikl. Mekh. Sib. Otd. Akad. Nauk SSSR, Novosibirsk, No. 7-84 (1984).
5. V. N. Vetlutskii and T. V. Poplavskaya, "Compressible laminar boundary layer on a flat triangular plate with an attached shock wave," Zh. Prikl. Mekh. Tekh. Fiz., No. 5 (1985).
6. L. C. Squire, "Flow regimes over delta wings at supersonic and hypersonic speeds," Aeronaut. Q., 27, No. 1 (1976).

7. G. I. Maikapar, "Separated flows on the leeward side of a delta wing and a solid of revolution in a supersonic flow," Uch. Zap. Tsentr. Aerogidrod. Inst., 18, No. 4 (1982)
8. L. G. Vasenev and A. M. Kharitonov, "Interference of a delta wing and a cylindrical body at supersonic velocity," Preprint, Inst. Teor. Prikh. Mekh. Sib. Otd. Akad. Nauk SSSR, Novosibirsk, No. 28-84 (1984).
9. K. Y. Narayan, "Leeside flowfield and heat transfer of a delta wing at M_∞ = 10," AIAA J., 16, No. 2 (1978).
10. A. K. Rastogi and W. Rodi, "Calculation of general three-dimensional turbulent boundary layers," AIAA J., 16, No. 2 (1978).
11. S. I. Shpak, "Calculation of a triangular incompressible turbulent boundary layer," Preprint, Inst. Teor. Prikl. Mekh. Sib. Otd. Akad. Nauk SSSR, No. 35-81 (1981),
12. B. M. Bulakh, Nonlinear Conical Gas Flows[in Russian], Nauka, Moscow (1970).
13. G. P. Voskresenskii, A. S. Il'ina, and V. S. Tatarenchik, "Supersonic flow about wings with an attached shock wave," Tr. TsAGI, No. 1590 (1974).
14. W. J. Bannik and C. Nebbeling, "An experimental investigation of the expansion flow field over a delta wing at supersonic speed," Rept/Delft Univ. Technol., VTH-167, Netherlands (1971).
15. K. C. Wang, "On the determination of zones of influence and dependence for three-dimensional boundary-layer equations," J. Fluid Mech., 48, No. 2 (1971).
16. B. Roux and B. Forestier, "Analysis of a compressible laminar boundary layer on a yawed cone," AIAA J., 14, No. 8 (1976).
17. G. N. Dudin, "Finite-difference method of solving three-dimensional boundary-layer equations for the regime of strong viscous interaction," Tr. Tsentr. Aerogidrod. Inst., No. 2190 (1983).

SUPERSONIC FLOW OVER DELTA WINGS AND ELEMENTS OF STAR-SHAPED BODIES AT ANGLES OF ATTACK AND ROLL

O. N. Ivanov and A. I. Shvets

UDC 533.6.011.55+629.782.015.3

Since the sixties there has been widespread investigation of the flow over triangular delta wings (e.g., [1-3]). It has been shown theoretically and experimentally that at supersonic speed a delta wing has a larger L/D than an equivalent planar triangular wing. In addition to studies of flow over lifting surfaces the aerodynamic characteristics of star shapes have been investigated [4-6]. These shapes, whose elements can be considered as delta wings, have considerably less drag at supersonic speeds than equivalent axisymmetric bodies.

In flight conditions one can achieve a flow regime where the plane of the angle of attack does not coincide with the plane of symmetry of a star-shaped body. Asymmetrical flow over delta wings forms in some cases at angles of attack and roll and also where there is asymmetry of the original wing shape. There are very few papers dealing with asymmetric flow over delta wings. Possible asymmetric shock wave patterns on delta wings have been studied [7]; in investigations of slip flow over delta wings of vertex angle $\Lambda > 150°$ calculations of the pressure distribution and the aerodynamic characteristics have been combined with direct measurements of pressure, force and momentum at M = 7.8-15.5 [8].

This paper gives results of experiments on supersonic flow over delta wings at angles of attack and roll. In contrast with [8] we studied the flow over delta wings over a wide range of vertex angle (Λ is the angle between the wetted surfaces of the delta wing) with both a curved shock wave, and with a shock system positioned between the wings, corresponding to Mach and regular interaction. At large vertex angles (Λ = 150-180°) the flow systems studied show flow asymmetry of a vehicle with delta wings, and for values of vertex angle ($\Lambda < 90$) they show flow over an element of a star-shaped body.

1. Experimental Technique and Model Description. Tests were made in a short-duration wind tunnel of the Institute of Mechanics, MGU. The aerodynamic facility has a closed

Moscow. Translated from Zhurnal Prikladnoi Mekhaniki i Tekhnicheskoi Fiziki, No. 1, pp. 81-87, January-February, 1989. Original article submitted November 9, 1987.

